BNL-64952

RESPONSE OF STRUCTURAL MATERIALS TO RADIATION ENVIRONMENTS*

CONF-970201--

C. J. Czajkowski

Brookhaven National Laboratory

Upton, NY, 11973-5000

USA

Abstract

An evaluation of proton and neutron damage to aluminum, stainless steel, nickel alloys, and various aluminum alloys has been performed. The proton studies were conducted at energies of 200 MeV, 800 MeV, and 23.5 GeV. The proton studies consisted of evaluation and characterization of proton-irradiated window/target materials from accelerators and comparison to nonirradiated archival materials. The materials evaluated for the proton irradiations included 99.9999 wt% aluminum, 1100 aluminum, 5052 aluminum, 304 stainless steel, and inconel 718. The neutron damage research centered on 6061 T-6 aluminum which was obtained from a control-rod follower from the Brookhaven National Laboratory's (BNL) High Flux Beam Reactor (HFBR). This material had received thermal neutron fluence up to ~4 x 10^{23} n/cm^2. The possible effects of thermal-to-fast neutron flux ratios are discussed. The increases in tensile strength in the proton-irradiated materials is shown to be the result of atomic displacements. These displacements cause interstitials and vacancies which aggregate into defect clusters which result in radiation hardening of the materials. Production of gas (helium) in the grain boundaries of proton irradiated 99.9999 wt% aluminum is also discussed. The major factor contributing to the mechanical-property changes in the neutron-irradiated 6061 T-6 aluminum is the production of transmutation products formed by interactions of the aluminum with thermal neutrons. The metallurgical and mechanical-property evaluations for the research consisted of electron microscopy (both scanning and transmission), tensile testing, and microhardness testing.

Introduction

This research emphasized the effects of high-energy proton (200 MeV and above) on aluminum, stainless steel, and nickel alloys and neutron damage to 6061 T-6 aluminum.

Neutron Irradiations

The Brookhaven National Laboratory (BNL) High Flux Beam Reactor (HFBR) [1,2] is a heavy-water cooled and moderated research reactor. The HFBR vessel is one entirely welded structure constructed of type 6061 T-6 aluminum. The predominant impetus for the neutron damage studies was the evaluation of the HFBR material condition [3], after 25+ years of service.

During the time period that the HFBR was being designed, it was the common belief that fast neutrons were the principal cause of radiation-damage-induced material degradation. The available data at the time showed that 6061 T-6 aluminum in this heat-treated condition (fully age-hardened) to be essentially unaffected by fast (E>1 MeV) fluences up to 1.2 x 10^{21} n/cm^2 [4].

Over the operating years, a number of specimens were removed from the HFBR for surveillance purposes. An evaluation of the data generated from these investigations indicated a number of possible phenomena occurring. The first observation was that the ductility of the 6061 T-6 alloy appeared to reach a saturation minimum value of approximately 9% above 1.5 x 10^{23} n/cm^2 thermal fluence. This saturation level [3] was surmised to have occurred by a mechanism of silicon buildup without creation of a brittle phase in the grain boundary network. This silicon buildup (beyond the maximum 7% solubility maximum) was first identified by Farrell [5, 6] who suggested that silicon buildup could continue beyond the saturation point, after observing the silicon building up at the surfaces of internal voids in a 6061 T-6 alloy. Since 6061 T-6 initially contains approximately 1% magnesium (the majority of which has already reacted with the silicon during the age-hardening process), the formation of a brittle Mg_2Si grain-boundary phase was considered not likely to occur. The possible role of fast-neutron fluence on the strengthening of this alloy was also evaluated during these programs. The data suggested that a high fast fluence may have the effect of randomizing the locations of the Si

atoms [3] by providing pinning sites and, therefore, reduce their effect on the mechanical properties of the alloy. Thus, results obtained from this program led to the following conclusions regarding neutron damage to 6061 T-6 in the HFBR:

1) The principal radiation effects on the aluminum is developed by the thermal neutrons' transmuting the Al to Si.
2) The effects of radiation damage appear to saturate above 1.8×10^{23} n/cm^2 (thermal neutrons).
3) The available data generated from the analyses were insufficient to establish a minimum-ductility cut-off point.

Seven years later, another test program was initiated and a control rod follower (CRDF) was evaluated,"A-2" (A-2 designates the specific CRDF in the reactor). This investigation consisted of a more detailed study [7, 8, 9, 10] of the 6061 T-6 alloy with microstructural detailing of radiation effects.

Proton Irradiation

The Department of Energy (DOE) in it's effort to replace aging defense production reactors has been evaluating the possibility of using a linear proton accelerator for production of tritum. A materials test program, in support of this DOE effort, consists of evaluation and characterization of previously-proton-irradiated stainless steel, aluminum and nickel alloy window/target materials. Evidence of materials degradation through either microstructural or mechanical-property deterioration are to be investigated and evaluated. Comparison to archive specimen mechanical/microstructural properties are performed wherever possible.

Experimental Approach

Neutron Irradiation

1. An evaluation of CRDF "A-2" (removed from the HFBR) was performed. This work consisted of transmission electron microscopy and x-ray diffraction studies. These tests were conducted to characterize the mechanical properties of the irradiated materials and the corresponding microstructures associated with these properties. A brief description of findings from this investigation will be discussed.

Proton Irradiation

1. 99.9999 wt% pure aluminum which had cracked/fragmented in a 800-MeV proton beam was evaluated. Sections of this material and nonirradiated stock from the same lot were compared. A scanning electron microscopic (SEM) examination of the fracture surfaces was made in an attempt to determine the failure mode. Standard tensile/hardness/impact tests were performed (to the extent possible) on these specimens and compared to the archive stock available. A microstructural evaluation by TEM was performed and compared to archive material.
2. 5052 aluminum alloy available in the form of both irradiated (-10^{19} p/cm^2 at 200 MeV, REF) and unirradiated archival material were evaluated by mechanical testing/microstructural analysis. These data were compared to those in the literature. Microstructural comparisons provided a basis for material effects in a 200-MeV proton beam.
3. Inconel windows (15) which had been irradiated in the BNL - Brookhaven Linac Isotope Producer (BLIP) - with 200 MeV protons and had seen a current total of 23,166 μA-h each.
4. A stainless-steel (Type 304) window from BLIP which had received approximately 900,000 μA-h of 200- M e V proton irradiation.

Test Procedures

All quantitative measurements/attribute testing were covered by ASTM standard procedures wherever possible. Metallographic techniques utilized for cutting, grinding, or polishing and were governed by "good laboratory practice". Note: all cutting of the aluminum specimens were done on an oil-cooled cutting wheel to minimize heat production.

Quality Assurance

In all cases, quantitative measurements were made with calibrated (to NIST standards, if applicable) equipment. Written procedures governed quality related activities performed for this program. In all cases, test methods complied with (to the extent possible) national standards, ASTM/ASME, or equivalent.

Results

Neutron Studies

Evaluations performed by Oak Ridge National Laboratory [10] on specimens removed from CRDF A-2 included both chemical analyses for silicon (Si) content, transmission electron microscopy, and energy dispersive spectroscopy (EDS). These evaluations were conducted on wafers cut from the previously tested charpy impact and tensile test specimens [7,8,9]. These wafers were approximately 1.3 mm square by 0.4 mm thick.

The ORNL work [10] noted that the nonirradiated control material (6061 T-6 aluminum) consisted of equiaxed grains with some dislocations, inclusions and a fine acicular precipitate of Mg_2Si. Diffraction patterns from these precipitates disclosed multiple-spot arrays (characteristic of single crystals). The irradiated specimens examined also exhibited an equiaxed microstructure and some inclusions (similar in size and distribution to the unirradiated material). These inclusions were determined by EDS to consist of Al, Fe, Si, Ni, and Cr. Electron diffraction patterns of these inclusions, however, were diffuse

DISCLAIMER

rings, which indicated that the material had undergone a crystalline-to-amorphous phase transformation due to the irradiation environment. A high concentration of small, almost spherical particles, consisting primarily of silicon, was distributed throughout the grains [15]. These spherical particles replaced the original acicular Mg_2Si microstructure. There was no evidence of radiation-produced voids, although there were large noncontiguous flakes, or islands, of silicon-rich phase that occupied less than one-fifth of the grain-boundary area and displayed no diffraction spots. These flakes were in evidence on almost every grain boundary examined. Additionally, at each side of grain boundaries and around inclusions, denuded areas (devoid of the spherical particles) were in evidence on the irradiated specimens examined.

The ORNL evaluations indicated the possibility that the re-ordering temperature for the amorphous silicon-rich phase coincided with the temperature of irradiation [10] "...making the conditions borderline for survival of amorphization". This question regarding the stability of the amorphous phase led to subsequent heat treatments, X-ray diffraction studies and evaluation of additional HFBR specimens (note: these data are still being reviewed and will be presented in a subsequent paper.

Proton Irradiation Data

Tensile tests were performed on each of the various procured archival stock materials (5052 aluminum, 304 stainless steel, and nickel alloy 718). Additionally, microhardness measurements were made on the 5052 H24 aluminum,. Microhardness measurements were performed since the irradiated materials were in the form of thin sheets and this method of testing would ensure consistency of the measured data. Table 1 lists the results of the various tensile tests performed on the archival stock. Only one specimen of the 5052 aluminum was tested.

Table 2: Microhardness Test Results (KN)

Inconel 718	
EDM	Punch
225,225,235,238,227	227,238,243,252,235
Avg. 230 KN	
Avg. 239 KN	
304 Stainless Steel	
EDM	Punch
183,178,183,181,195,181	197,189,189,187,201
Avg. 184 KN	Avg. 193 KN
5 052 H24 Aluminum	
EDM	Punch
Material lost during cutting	34.5,39.4,53.7,37.8,42.7
	Avg. 41.6 KN

The microhardness data for each of the archival materials is tabulated in Table 2. Two sets of microhardness values were recorded for each material.

Scanning Electron Microscopy (SEM)

The fracture faces of each of the materials tensile tested were examined by SEM. This evaluation was used to determine the mode of fracture from the uniaxial tensile pulls. Figure 1 is the low-magnification fracture surface associated with the 304 stainless steel specimen. The fracture was of the dimpled rupture type (Figure 2) which is typical of a ductile material failure. Dimples are depressions in the microstructure and occur by a process of microvoid nucleation in areas of high plastic strain. Metallic inhomogeneities are preferred sites for this microvoid nucleation at grain boundaries. These microvoids grow (coalesce) as the strain increases, and finally rupture occurs, producing the dimpled rupture appearance.

Transmission Electron Microscopy (TEM)

For this project electrolytic thinning was employed using various etchants. A number of nonirradiated test specimens were thinned in order to develop the proper technique (thinning parameters) prior to use on irradiated material. After thinning, the various specimens were stored in partitioned containers and placed in designated containers. The specimens were then examined by TEM.

The stainless steel archive material was examined in the TEM. Figure 3 shows a deformation twin in the stainless steel with dislocations at the twin boundary. These microstructures are common in the 304 stainless steel, as well as the triple point (Figure 4) which was also noted in the 304 stainless archive material.

The matrix structure of the 5052 H24 alloy was also examined by TEM (Figure 5). Various precipitates were examined with two of the typical types having been further characterized by energy-dispersive spectroscopy (EDS).

EDS is an analytical technique capable of performing elemental analysis of microvolumes, typically on the order of a few cubic microns in bulk samples and considerably less in thinner sections.

Table I Tensile Test Results

Inconel 718

Specimen Number	Displacement at Peak (in)	% Strain at Peak (%)	Load at Peak (lbs)	Stress at Peak (psi)	Stress at 0.2% Yield (psi)	% Strain at Break (%)	Stress at Break (psi)
1	0.7370	58.96	327.4	131000.	64360.	62.48	126100.
2	0.7061	56.48	325.2	130100.	63310.	61.84	121200.
Mean	0.7215	57.72	326.3	130500.	63840.	62.16	123600.
Standard Deviation	0.0219	1.75	1.6	623.	744.	.45	3479.

304 Stainless Steel

Specimen Number	Displacement at Peak (in)	% Strain at Peak (%)	Load at Peak (lbs)	Stress at Peak (psi)	Stress at 0.2% Yield (psi)	% Strain at Break (%)	Stress at Break (psi)
Excluded	0.9611	76.89	270.6	130700.	43900.	82.49	96020.
2	0.9589	76.71	267.8	102600.	42750.	84.31	96320.
Excluded	0.9481	75.85	268.6	102900.	42000.	85.61	98540.
Mean	0.9589	76.71	267.8	102600.	42883.	84.31	96320.
Standard Deviation	—	—	—	—	—	—	—

5052 H24 Aluminum

Specimen Number	Displacement at Peak (in)	% Strain at Peak (%)	Load at Peak (lbs)	Stress at Peak (psi)	Stress at 0.2% Yield (psi)	% Strain at Break (%)	Stress at Break (psi)
	0.185	—	46.0	46,000	—	—	—
Mean	—	—	—	—	—	—	—
Standard Deviation	—	—	—	—	—	—	—

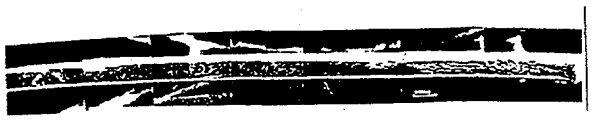

Figure 1: Low-magnification fractograph of 304 stainless steel

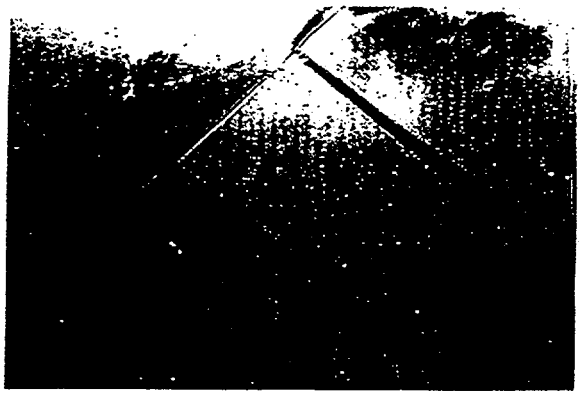

Figure 3: A deformation twin is seen in this TEM photo of unirradiated 304 stainless steel.

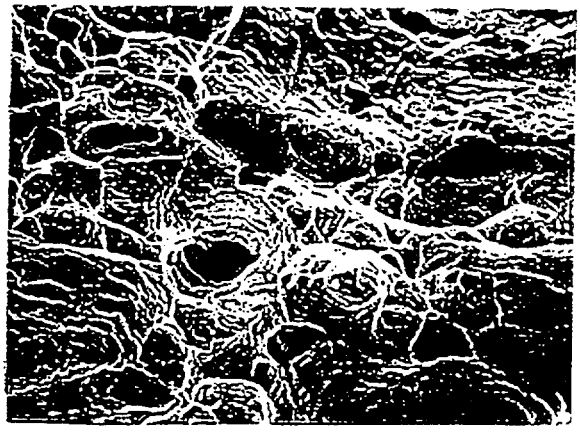

Figure 2: Higher-magnification SEM photo showing ductilefailure (typical).

Figure 4: A triple point is seen in the austenitic matrix of the unirradiated 304 stainless steel.

Analysis of X-rays emitted from a sample is accomplished by crystal spectrometers which use energy dispersive spectrometers and permit analysis by discriminating among X-ray energies. (Note: EDS will only discern elements with atomic numbers greater than Na so certain light elements will not be detected.) The precipitates examined by EDS were determined to be primarily composed of silicon and iron.

Irradiated Material Examination

5052 H24 REF Windows

Specimens of 5052 H24 aluminum REF (Radiation Effects Facility) windows (irradiated with 200-MeV protons to a fluence of ~2 x 10^{19} p/cm^2) were EDM machined in the shape

Figure 5: Matrix structure of 5052 H24 Aluminum archival stock.

Figure 7: TEM photo of grain boundary in irradiated 5052 Aluminum. Small cavities seen in the grain boundary. [36,000X].

Figure 6: Fractograph of 5052 H24 Aluminum window after irradiation (ductile).

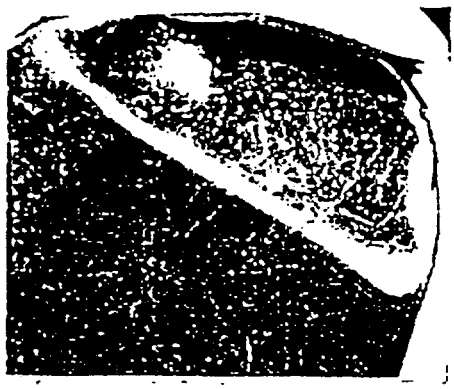

Figure 8: Damage to BLIP windows seen in this photograph.

of tensile specimens and then uniaxially tensile tested. Table 3 is the tabulation of these results. Figure 6 shows that the fracture face associated with the irradiated 5052 H24 aluminum is similar in appearance to those of the unirradiated archive material (i.e., ductile). This similarity in appearance is also reflected in the similar tensile strengths and elongations noted in Table 4. There was a reduction in tensile strength (~7%) concurrent with a reduction in total elongation (~9%). It is very difficult to take these reduced values at face value without considering the very small loadings (19.5 and 20.9 kg) needed to fracture these specimens.

TEM evaluations of the irradiated 5052 aluminum specimens disclosed some evidence of cavity and gas formation in the grain boundaries (Figure 7). There was some evidence of dislocations in the metal matrix. This possible gas formation was the result of proton interactions with the aluminum in the 200-MeV beam.

Figure 9 Cracking is evident in this photograph of a BLIP window

Brookhaven Linac Isotope Producer (BLIP) Windows

304 StainlessSteel and Alloy 182 Examination

Fifteen windows (6 stainless steel and 9 Inconel) were obtained from the BLIP facility. The BLIP facility was first operated in 1973. It was the world's first facility to demonstrate the use of a large proton Linac to produce medical radionuclides efficiently. This production of radioisotopes was accomplished by proton spallation and lower energy reactors. The BLIP facility uses excess beam capacity from a proton Linac (200 MeV) which is injected into the 33 MeV Alternating Gradient Synchrotron (AGS). Spallation reactions produce nuclides with mass numbers less than the target.

It is evident that there was a dramatic increase in microhardness with the proton irradiations. Due to bends or cracks, specimens were unable to be machined from all windows (for this report).

Table 3 lists the microhardness readings obtained (average of 5), the flux of protons, and the corresponding unirradiated microhardness readings obtained from the previous EDM machined microhardness specimens.

The "as received" windows were in various conditions, ranging from good to poor. Good windows provided meaningful mechanical property test results because they were relatively flat and free from defects which interfered cutting . Figures 8 and 9 are photographs of two of the windows. The defects noted on these windows ranged from the window being bent, pitted, grooved and one of the windows had severe cracking in evidence. If "usable" materials were available, one tensile and

Table 3: Irradiated Microhardness Measurements (Avg. of 5 readings)

Specimen I. D.	Microhardness (KN)	Nonirradiated Microhardness (KN)	Fluence (μAh)
IN KQ-1	---	230.0	28,540.8
IN KQ-2	2276.6	230.0	28,540.8
IN LI-1	308.0	230.0	23,166.6
IN LI-2	319.0	230.0	23,166.6
IN. JH	317.7	230.0	10,248.4
IN LA-1	---	230.0	23,166.6
IN LA-2	---	230.0	23,166.6
IN LD	---	230.0	23,166.6
IN KD	---	230.0	28,540.8
SS KL-1	267.6	184.0	3,919.5
SS KL-2	265.1	184.0	3,919.5
SS KD-1	302.3	184.0	6,781.1
SS KD-2	---	184.0	6,781.1
SS DH-1	---	184.0	4,250.0
SS DH-2	---	184.0	4,250.0

Figure 10: Specimen layout (typical) for TEM and tensile specimens.

four TEM size (Figure 10). One of the TEM slices was mounted for microhardness measurements, one was thinned for TEM examination, and two were labelled and kept for archive material. Note: The location of the area of greatest proton flux was determined by placing a photographic film (Polaroid) over

the window and then developing it. The area of greatest activity (lightest area) determined where the EDM cuts were made.

Discussion and Conclusions

5052 Aluminum

The 5052 aluminum material showed a reduction in tensile strength after irradiation with 200-MeV protons. This result was considered surprising since proton irradiation would normally increase the tensile strength of the 5052 by a displacement/hardening mechanism. This phenomenon had been seen previously, however, with irradiations by 800-MeV protons [12, 13]. These irradiations were done at ~50°C, to doses of 0.2 dpa (3.2 x 10^{20} p/cm^2) on 6061 and 5052 cold-worked aluminum. These results were in clear disagreement with expected results for 5052 aluminum, and results on 6061 aluminum irradiated to much higher doses [14] (up to 260 dpa). This evaluation [12, 13] suggested that the main cause of the radiation-induced loss of strength was due to a loss of cold work in the 5052 material (radiation-induced), and a reduction of Mg_2Si precipitates in the 6061 aluminum. A dissolving of the precipitates (6061) under 800-MeV radiation conditions at low dose was considered (by the Los Alamos researchers) to be the main cause of the softening.

Table 4: Results of Tensile Testing of Window Materials

5052 H24 Aluminum (0.010-cm thickness)

	Tensile Strength (psi)	Load (lbs.)	Total Elongation (in.)
Irradiated	43,000	43.0	0.150
Unirradiated	46,000	46.0	0.165

Stainless Steel (0.025-cm thickness)

	Tensile Strength (psi)	Load (lbs.)	Total Elongation (in.)
Unirradiated	108,000	270.0	0.920
Unirradiated	105,600	264.0	0.995
Irradiated (KL-2)	116,400	291.0	0.945
Irradiated (KD-1)	119,200	298.	0.920
Irradiated (KL-1)	117,600	294.0	0.640

Inconel (0.25-cm thickness)

	Tensile Strength (psi)	Load (lbs.)	Total Elongation (in.)
Unirradiated	127,200	318.0	0.695
Unirradiated	127,200	318.0	0.630
Irradiated (LI-2)	109,200	273.0	0.170
Irradiated (LI-1)	151,200	378.0	0.480
Irradiated (JH)	135,600	339.0	0.375

This loss of cold-worked microstructure would be a plausible explanation for the loss of strength. The original Los Alamos hypothesis [12, 13] of this phenomenon has since been re-evaluated (by the Los Alamos researchers). The current [15], more plausible explanation for the material softening was precipitate coarsening and over-ageing due to beam heating well in excess of the anticipated temperatures. This explanation is also considered to be a distinct possibility in our study. This REF window was subjected to 200-MeV protons without temperature controls or temperature monitoring. These temperatures are assumed to be sufficiently high enough to anneal out dislocations and subsequently soften the 5052 alloy.

Neutron-Irradiated 6061 T-6 Aluminum

The effects of fast-neutron displacement damage and transmutation effects in 6000 series aluminum have been extensively investigated by various researchers [5, 16-25]. This body of work, coupled with additional research on 99.9999 wt% [26-33], 1100 aluminum [46, 34-40] and 5000 series aluminum [41, 42, 43], make up the bulk of information on neutron effects in aluminum and its alloys.

Some of the earliest work on the effect of thermal neutrons on aluminum alloys was performed at ORNL [33, 35, 38, 40]. These studies determined that silicon is produced in aluminum through the ^{27}Al (n,γ) ^{28}Al, ^{28}Al-^{28}Si+β reactions mostly through the interaction with thermal neutrons, and that fast neutron interactions caused the formation of dislocation loops and eventually, voids [32, 43].

The development of silicon-rich amorphous phases in the HFBR alloy is interesting because radiation-induced amorphization does not occur in simple metals, but is normally limited to semiconductors and ceramic compounds (e.g., Si). For the amorphous condition to exist, the temperature of irradiation must be lower than the temperature at which re-ordering of the crystal lattice atoms occurs. This re-ordering can take place at temperatures below those of bulk diffusion in the alloy. An amorphous silicon-rich phase has been previously recorded in 1100 aluminum [35]. This prior investigation reported crystalline silicon-rich precipitate particles in the matrix of 1100 aluminum with the co-existence of amorphous silicon-rich coatings around radiation induced voids. An area for future study

would be the systematic determination of the reordering temperature for the HFBR irradiation-produced silicon-rich phase. This exercise would entail the extraction of the amorphous precipitate phase from the bulk material. Determination of the amorphous phase mechanical properties would also be both challenging and interesting. For instance, is the phase ductile or brittle? How do it's properties compare to the crystalline phase? Questions well worth investigating if funds and programs allow.

The existence of precipitate-free zones (PFZs) in the irradiated HFBR material has been observed in over-aged nonirradiated 6XXX aluminum [44]. The development of PFZs (after slow quenching and aging) is caused by the depletion of solute atoms near the particles or grain boundaries and to the lack of nucleation sites caused by the migration of vacancies to particle-matrix boundaries during the quench. Grain-boundary precipitation is often accompanied by the development of PFZs [44] similar to that observed adjacent to dispersoid particles. Dispersoid particles affect quench-sensitive precipitation since they both modify the dislocation structure of the quenched material and act as nucleation sites for precipitation.

The appearance of spherical silicon-rich particles in the irradiated HFBR aluminum is interesting. One possible explanation for their shape is that they are not spherical at all, and that the TEM is not sensitive enough to resolve any angular facets of their construction that might be present. Another possibility for their shape is related to the aging process itself. The 6XXX series aluminum alloys strengthen over a long period of time at room temperature This strengthening requires the formation of GP zones. Since Mg_2Si may originally exist in a spherical form, radiation could be simply causing an enhanced diffusion of the precipitate back to this form. This spherical form of the silicon-rich particles is probably compositionally dependent.

TEM investigations associated with a study of 5052 aluminum [32] disclosed no irradiation-induced voids in the material after a fast-neutron fluence of 1.1×10^{22} n/cm^2 (> 0.1 MeV). Later investigations by ORNL [38] determined that irradiation-induced strengthening in 5052 aluminum was due to irradiation-produced Mg_2Si precipitates. This indicated that thermal-neutron-fluence transmutation effects were the primary cause of strengthening this aluminum alloy. Further work by Farrell [42] on this alloy added additional information on the irradiation damage effects on 5052 aluminum. Farrell determined that mixed-spectrum irradiations on the 5052 at 328 K converts the alloy to a precipitation hardened 6000 series type alloy whose precipitates are developed by transmutation-produced silicon. It was also noted that increasing the thermal-to-fast neutron flux ratio from 1.7 to 2.1 imparted additional strengthening beyond the expectations of the silicon increase. This increased strengthening was attributed to the fineness of the irradiation-induced precipitate which was finer than that produced by thermal aging in a 6061 alloy. The increase in additional strength was surmised to be the result of higher silicon production at the 2.1 thermal/fast fluence, causing both faster production and finer Mg_2Si particles.

BLIP Windows

The irradiated windows (both stainless and Inconel), with the exception of Inconel window LI-2, all exhibited an expected increase in tensile strength with proton irradiation. Microhardness values for all of the windows tested also increased, again as expected. There were no new failure mechanisms observed on any of the windows examined. Further investigations of windows LI-2, and KL-1 (stainless window) will continue during the next calendar year.

Acknowledgments

*Work supported under US DOE Contract DE-AC02-76CH00016.

REFERENCES

1. Memo: Revised Fast and Thermal Fluences for Radiation Damage Estimates, P. Tichler, (April, 1985).

2. BNL-24182, Revised, HFBR Handbook, October 1992.

3. Weeks, J.R., Czajkowski, C.J., and Tichler, P.R., ASTM 1046, Effects of Radiation on Materials: 14th International Symposium (Vol. II), 1990, 441-452.

4. Graber, M.J., and Ransick, J.H., "ETR Damage Surveillance Programs, Progress Report 1", January 27, 1961.

5. Farrell, K., and King, R.T., "Tensile Properties of Neutron-Irradiated 6061 Aluminum Alloy in Annealed and Precipitation-Hardened Conditions", ASTM STP 683, Effects of Radiation on Structural Materials, 1979, 440-449.

6. Farrell, K., "Radiation Response of Aluminum and its Alloys After Exposure in the High Flux Isotope Reactor", Presented at AIME Annual Meeting, Chicago, IL, March 1981.

7. Czajkowski, C.J., Schuster, M.H., Roberts, T.C., and Milian, L.W., "Tensile and Impact Testing of a HFBR Control Rod Follower", BNL Informal Report BNL-43367.

8. Czajkowski, C.J., "Fractography Evaluation of Impact and Tensile Specimens from the HFBR", BNL Informal Report BNL-43602.

9. Czajkowski, C.J., Schuster, M.H., and Roberts, T.C., "Tensile Testing and Scanning Electron Microscope Examination of Charpy Impact Specimens from the HFBR", BNL Informal

Report, BNL-43843.

10. Farrell, K., "Microstructural Appraisal of a HFBR Control Rod Follower Tube", Letter Report, February 26, 1990.

11. Weeks, J.R., Czajkowski, C.J., and Farrell, K., "Effects of High Thermal Neutron Fluences on Type 6061 Aluminum", ASTM STP 1175 Effects of Radiation on Materials: 16th International Symposium, 1993, 1168-1182.

12. Singh, B.N., Lohmann, W., Ribbens, A., and Sommer, W.F., "Microstructural Changes in Commercial Aluminum Alloys Caused by Irradiation with 800-MeV Protons", ASTM STP 955, Radiation Induced Changes in Microstructure: 13th International Symposium (Part 1), 1987, 508-519.

13. Lohmann, W., Ribbens, A., Sommer, W.F., and Singh, B.N., "Microstructure and Mechanical Properties of Medium Energy (600-800 MeV) Proton Irradiated Commercial Aluminum Alloys", Radiation Effects, 1986, Vol. 101, 283-299.

14. Wechsler, M.S., Stubbins, J.F., Sommer, W.F., Ferguson, P.D., and Farnum, E.H., "Selection and Qualification of Materials for the Transmutation of Waste Project", Los Alamos Report, LA-UR-92-1211, 1992.

15. Ullmaier, H., and Carsughi, F., "Radiation Damage Problems in High Power Spallation Neutron Sources", Nuclear Instruments and Methods in Physics Research B 101, 1995, 406-421.

16. McCoy, H.E., Jr., and Weir, J.R., Jr., "Influence of Irradiation on the Tensile Properties of the Aluminum Alloy 6061", Nuclear Science and Engineering, 25, 1966, 319-327.

17. Sturcken, E.F., "Irradiation Effects in Magnesium and Aluminum Alloys", Savannah River Laboratory Report, DP-MS-78-31, 1978.

18. Farrell, K., Long, E.L., King, R.T., and Jostons, A., "Postirradiation Examination and Testing of the ORR N_F Tray", Oak Ridge National Laboratory Report, ORNL-TM-4183, June 1973.

19. Alexander, D.J., "The Effect of Irradiation on the Mechanical Properties of 6061-T651 Aluminum", ASTM STP 1175, Effects of Radiation on Materials: 16th International Symposium, ASTM, 1993, 1151-1167.

20. Farrell, K., "Assessment of Aluminum Structural Materials for Service Within the ANS Reflector Vessel". Oak Ridge National Laboratory Technical Report, ORNL/TM-13049, August 1995.

21. King, R.T., Jostons, A., Farrell, K., "Neutron Irradiation Damage in a Precipitation-Hardened Aluminum Alloy", ASTM STP 529, Effects of Radiation on Substructure and Mechanical Properties of Metals and Alloys, 1973, ASTM, 165-179.

22. Farrell, K., "New Findings in Radiation Damage in Aluminum Alloys", Presentation to the AERO Engr./Tech. Working Group, Aiken, SC, 1/16/91.

23. Farrell, K., and Richt, A.E., "Postirradiation Properties of the 6061-T6 Aluminum High Flux Isotope Reactor Hydraulic Tube", ASTM STP 570, Properties of Reactor Structural alloys after Neutron or Particle Irradiation, ASTM, 1976, 311-325.

24. Sturken, E.F., Krapp, C.W., and Alewine, G.B., "Effects of Irradiation on 6063 Aluminum Structural Components in Savannah River Reactors", Symposium on Materials Performance in Operating Nuclear Systems, August 28-30,1973, Ames, Iowa.

26. Schule, W., "Radiation-Enhanced Diffusion in Face-Centered Cubic Materials", Proceedings of the 10th International Symposium on Effects of Radiation on Materials, Savannah, GA, June 1980, 167-177.

26. Packan, N.H., "Voids in Re-Irradiated Aluminum", J. Of Nuclear Materials, 37, 1970, 251-254.

27. Packan, N.H., "Fluence and Flux Dependence of Void Formation in Pure Aluminum", J. Of Nuclear Materials, 40, 1971, 1-16.

28. Wolfenden, A., "Damage in Aluminum by 200 kV Electrons", J. Of Nuclear Materials, Letters to the Editors, 1971, 114-115.

29. Houston, J. T., and Farrell, K., "Void Coarsening in High Purity Aluminum During Postirradiation Annealing", J. Of Nuclear Materials, 40, 1971, 225-229.

30. Farrell, K., and King, R.T., "Supervoids in Irradiated Aluminum", Phys. Stat. Sol. (A) 2, K5, 1970.

31. Stiegler, J.O., Farrell, K., Dubose, C.K.H., and King, R.T., "High-Fluence Neutron-Irradiation Damage in Aluminum", IAEA-SM-120/F-5.

32. Horsewell, A., and Singh, B.N., "Influence of Grain and Subgrain Boundaries on Void Formation and Growth in Aluminum Irradiated with Fast Neutrons", ASTM STP 955, Radiation-Induced Changes in Microstructure: 13th International Symposium, 1987, 220-229.

33. Farrell, K., Wolfenden, A., and King, R.T., "The Effects of Irradiation Temperature and Preinjected Gases on Voids in Aluminum", Radiation Effects, Vol. 8, 1971, 107-114.

34. Ceresara, S., Federighi, T., and Pieragostini, F., "Recovery

of Al-Si Alloys Neutron Irradiated at 78 Degrees K", Phys. Stat. Sol., 11, 1965, 779-787.

35. Farrell, K., Bentley, J., and Braski, D.N., "Direct Observation of Radiation-Induced Coated Cavities", Scripta Metallurgica, Vol.11, 1977, 243-248.

36. Wolfenden, A., "Effects of Preinjected Hydrogen on the Electron Displacement Damage in 1100 Aluminum", J. Of Nuclear Materials, 40, 1971, 351-352.

37. Farrell, K., and Richt, A.E., "Microstructure and Tensile Properties of Heavily Irradiated 1100-0 Aluminum", ASTM STP 683, Effects of Radiation on Structural Materials, 1979, 427-439.

38. Farrell, K., and King, R.T., "Radiation-Induced Strengthening and Embrittlement in Aluminum", Met. Trans., 4, May 1973, 1223-1231.

39. Jostons, A., and Long, E.L., Jr., "Radiation Damage and the Effects of Postirradiation Annealing in 1100 Grade Aluminum", Radiation Effects, Vol.16, 1972, 83-94.

40. Farrell, K., Steigler, J.O., and Gehlbach, R.E., "Transmutation-Produced Silicon Precipitates in Irradiated Aluminum," Metallography, 3, 1970, 275-284.

41. Singh, B.B., Horsewell, A., Sommer, W.F., and Lohmann, W., "Gas Accumulation at Grain Boundaries During 800-MeV Proton Irradiation of Aluminum and Aluminum Alloys", J. Of Nuclear Materials, 141-143, 1986, 718-722.

42. Zhang, Y.G., and Jones, I.P., "Electron Irradiation of Aluminum-Zinc Alloys, 1. Radiation-Induced Segregation in an Aluminum-0.35 at% Zinc Alloy", J. Of Nuclear Materials, 165, 1989, 252-265.

43. Brimhall, J.L., and Mastel, B., "Voids in Neutron Irradiated Face Centered Cubic Metals", J. Of Nuclear Materials, 29, 123-125.

44. Aluminum:Properties and Physical Metallurgy , Edited by: Hatch, J.E., 1984, American Society for Metals.

63. Farrell, K., "Microstructure and Tensile Properties of Heavily Irradiated 5052-0 Aluminum Alloy", J. Of Nuclear Materials, 97, 1981, 33-43.